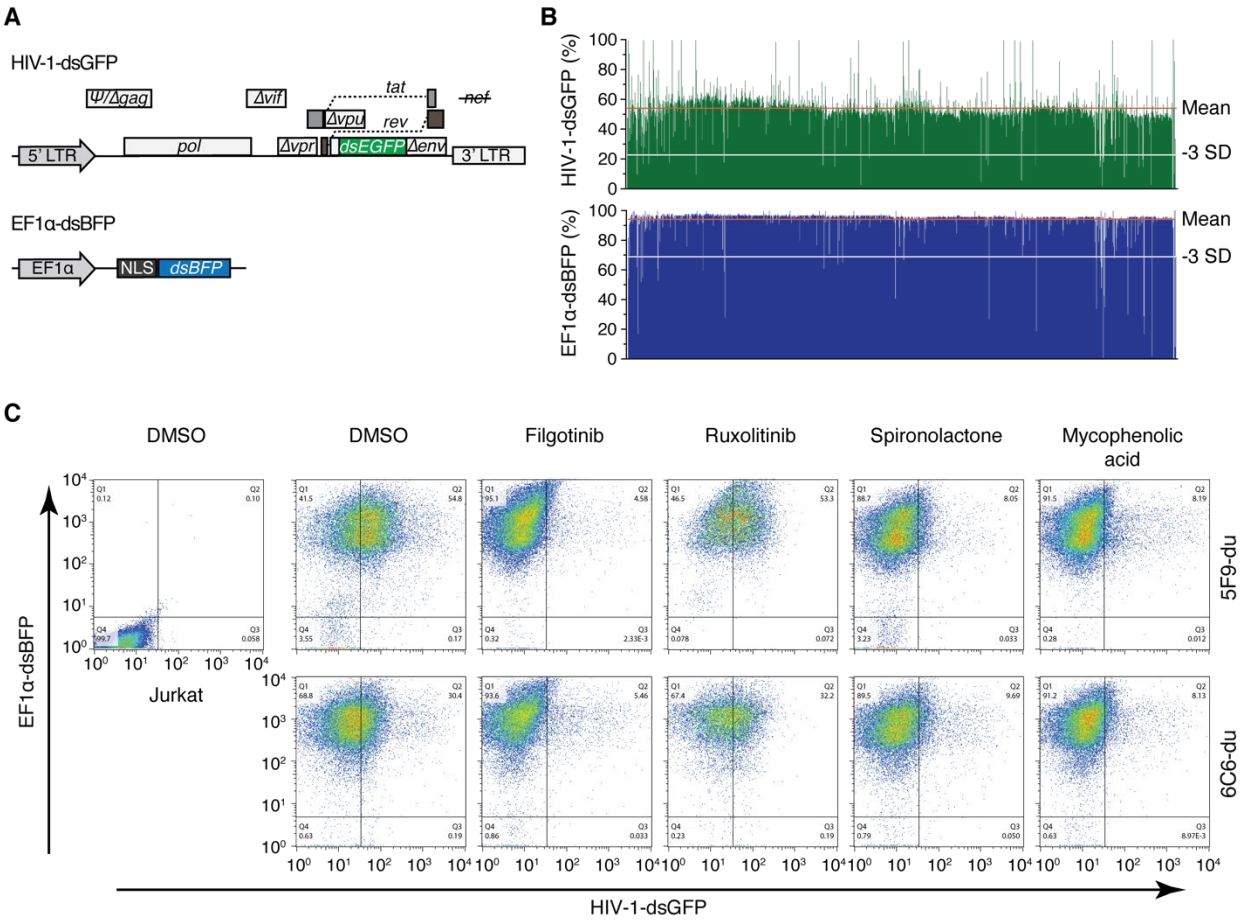

Figure S1. An FDA-approved small molecule compound library screen identified HIV-1-suppressing agents. (**A**) Scheme of the lentiviral reporter constructs. The HIV-1-dsGFP reporter has an NL4-3-EGFP-derived full-length HIV-1 provirus which preserves HIV-1 splice sites and cis-acting elements such as TAR and RRE. Six inactivating mutations were introduced into *gag*, *vif*, *vpr*, *vpu* with truncated *nef* and deleted *env* to reduce cellular toxicity (42). Both dsGFP and dsBFP are targeted for rapid degradation through the PEST sequence, resulting in a short half-life of 2 hours (42) and thus a real-time reflection of HIV-1-driven dsGFP and EF1α-driven dsBFP expression. We separated dsGFP and dsBFP in different cellular compartments to avoid fluorescent resonant energy transfer (FRET) between dsBFP and dsGFP: the dsGFP is targeted into the endoplasmic reticulum through the signal peptide leader sequence, while the

dsBFP is targeted into the nucleus by a nuclear localization signal (NLS). (**B**) A small molecule compound library of 1,430 FDA-approved drugs (10 μM) were screened in 96-well plates with dual color Jurkat clone 1B6-du (integration site *ITGAE*) for 24 hours. In each 96-well plate, four wells of flavopiridol served as positive controls and four wells of DMSO served as negative controls. Drugs which can suppress HIV-1-dsGFP expression three standard deviations below mean without reducing EF1α-driven dsBFP expression for more than three standard deviations below mean were considered as candidate HIV-1-suppressing agents for further evaluation. (**C**) Representative flow cytometry plots of dual reporter HIV-1-infected Jurkat clones 5F9-du and 6C6-du treated with 10 μM HIV-1-suppressing agents for 24 hours. GFP, green fluorescent protein. BFP, blue fluorescent protein. NLS, nuclear localization signal.

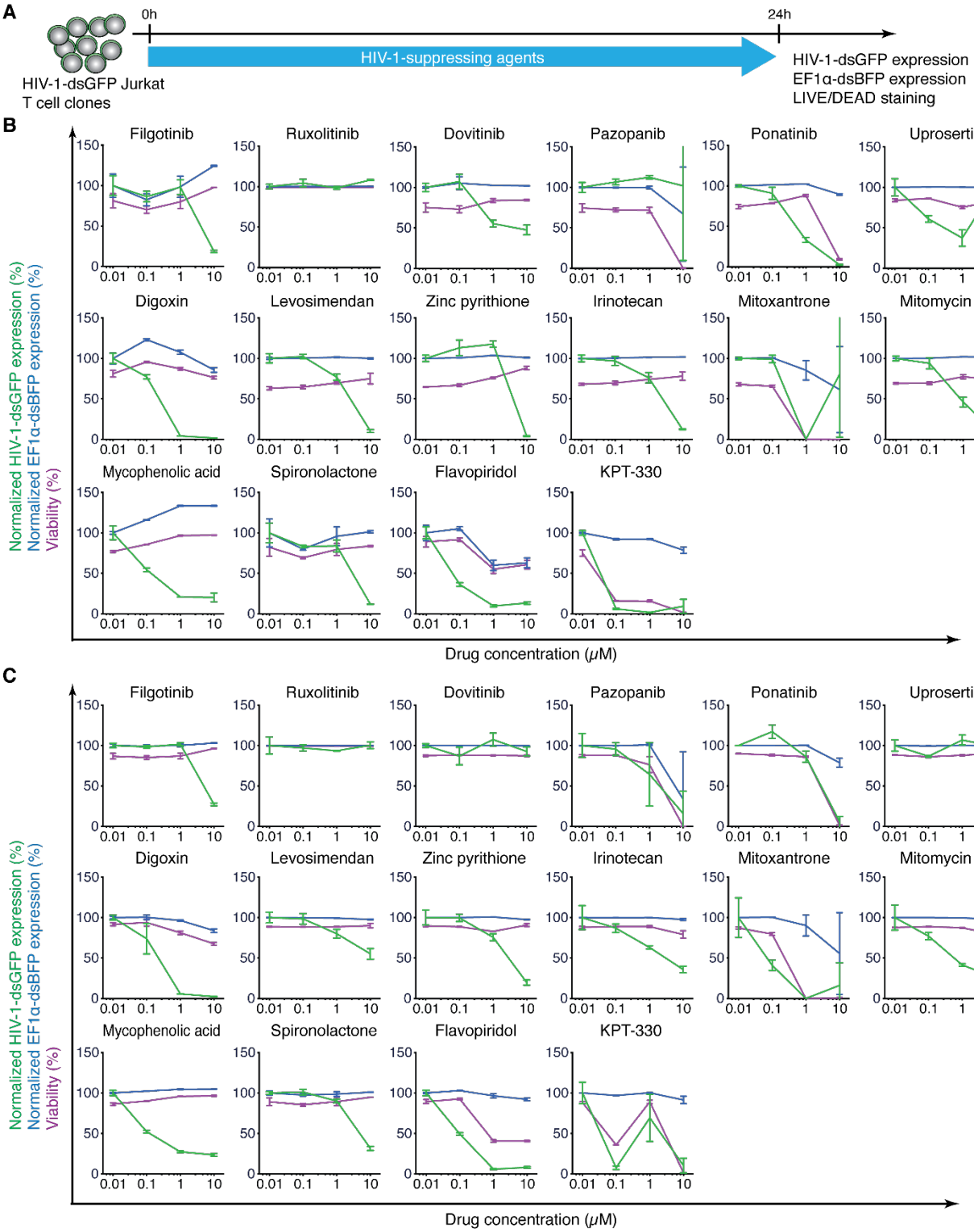
A
0h
24h
HIV-1-suppressing agents
HIV-1-dsGFP Jurkat
T cell clones
HIV-1-dsGFP expression
EF1α-dsBFP expression
LIVE/DEAD staining
B
C
Filgotinib
Ruxolitinib
Dovitinib
Pazopanib
Ponatinib
Uprosertib
Digoxin
Levosimendan
Zinc pyrithione
Irinotecan
Mitoxantrone
Mitomycin C
Mycophenolic acid
Spironolactone
Flavopiridol
KPT-330
Normalized HIV-1-dsGFP expression (%)
Normalized EF1α-dsBFP expression (%)
Viability (%)
Drug concentration (μM)

Figure S2. Dose response curves and viability measurement using dual-color HIV-1-infected Jurkat clones treated with HIV-1-suppressing agents. (**A**) Schematic presentation of the experimental design. (**B–C**) Dose response curves of HIV-dsGFP, EF1α-dsBFP, and viability of (**B**) HIV-1-infected Jurkat 5F9-du (integration site *INPPL1*) and (**C**) HIV-1-infected Jurkat 6C6-du (integration site *PLGLB1*) for 24 hours. The expression levels were normalized to that of DMSO-treated controls.

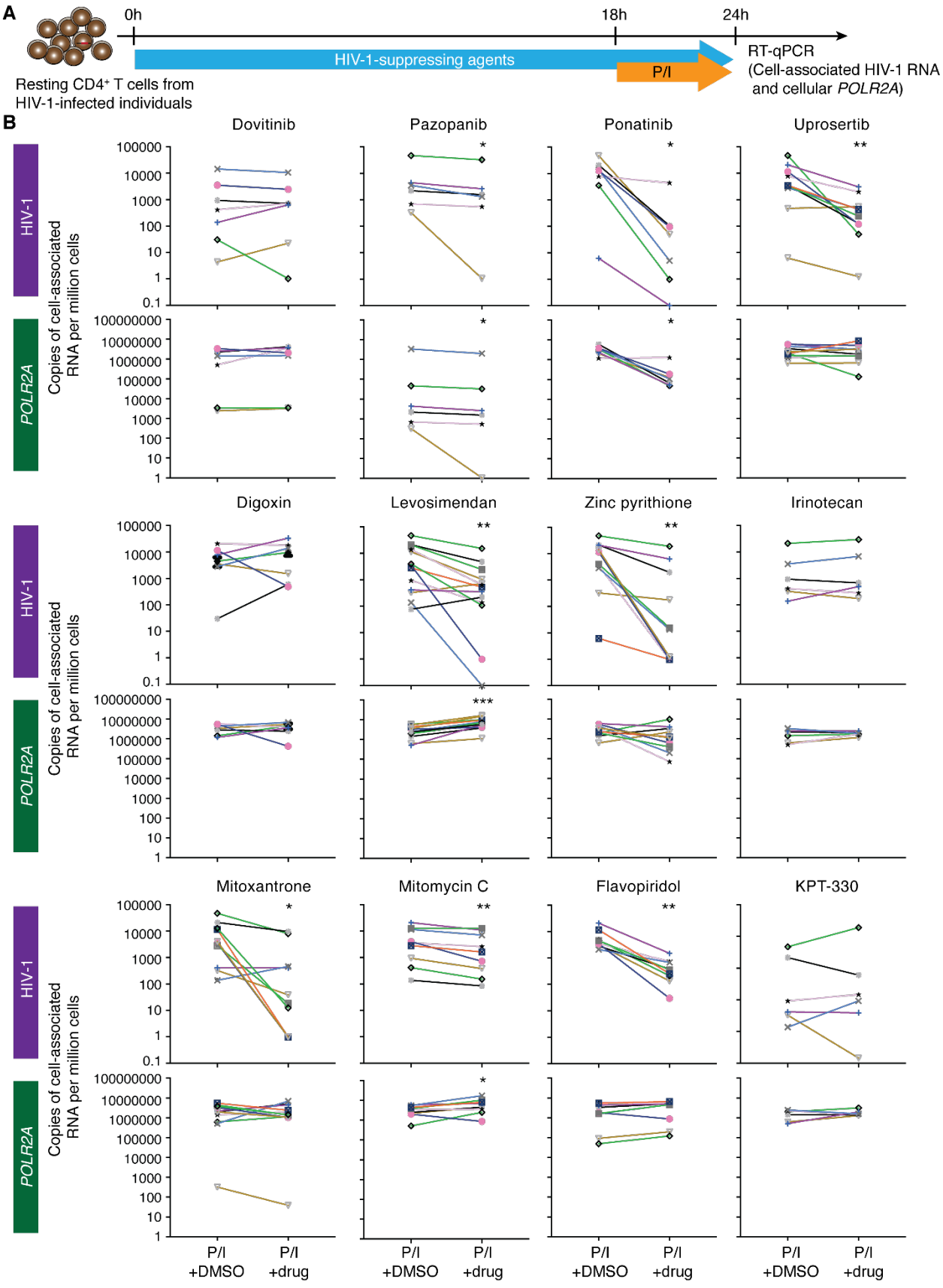
A
0h
18h
24h
HIV-1-suppressing agents
P/I
RT-qPCR
(Cell-associated HIV-1 RNA
and cellular POLR2A)
Resting CD4+ T cells from
HIV-1-infected individuals
B
Dovitinib
Pazopanib
Ponatinib
Uprosertib
Digoxin
Levosimendan
Zinc pyrithione
Irinotecan
Mitoxantrone
Mitomycin C
Flavopiridol
KPT-330
HIV-1
POLR2A
Copies of cell-associated
RNA per million cells
P/I
+DMSO
P/I
+drug

Figure S3. Cell-associated RNA levels of polyadenylated HIV-1 and a housekeeping gene *POLR2A* of candidate HIV-1-suppressing agents. (**A**) Schematic representation of the experimental design. (**B**) Cell-associated RNA levels of polyadenylated HIV-1 and a housekeeping gene *POLR2A* in $CD4^+$ T cells from virally suppressed, HIV-1-infected individuals upon treatment with HIV-1-suppressing agents (10 μM) for 24 hours and PMA/ionomycin challenge during the final 6 hours in the presence of ART (1 μM of tenofovir and 10 μM enfuvirtide). Each color represents one HIV-1-infected individual. P/I, PMA/ionomycin. *, $P < 0.05$; **, $P < 0.01$; ***, $P < 0.001$ by two-tailed Wilcoxon rank sum test.

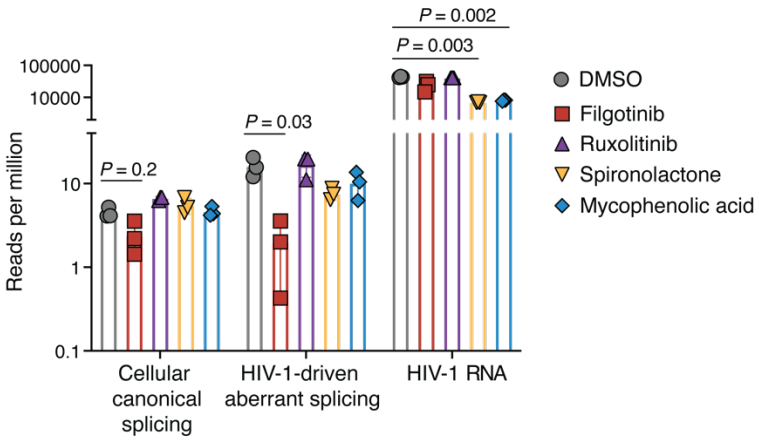

Figure S4. Effect of HIV-1-suppressing agents on host, HIV-1-to-host and HIV-1 RNA splicing in HIV-1-infected Jurkat clone 8B10. To examine the effect of HIV-1-suppressing agents on RNA splicing, we examined cellular canonical splicing (from *VAV1* exon 1 to *VAV1* exon 2), HIV-1-to-host aberrant splicing (from HIV-1 major splice donor site to *VAV1* exon 2), and HIV-1 RNA expression (total HIV-1 RNA). Reads were normalized to total mapped reads and presented as reads per million total reads. Analysis was performed using the same triplicated RNA-seq data for each treatment as described in Figure 4. *P* values were calculated using repeated measures two-way ANOVA with Geisser-Greenhouse correction and *post hoc* analysis with Dunnett's multiple comparisons test.

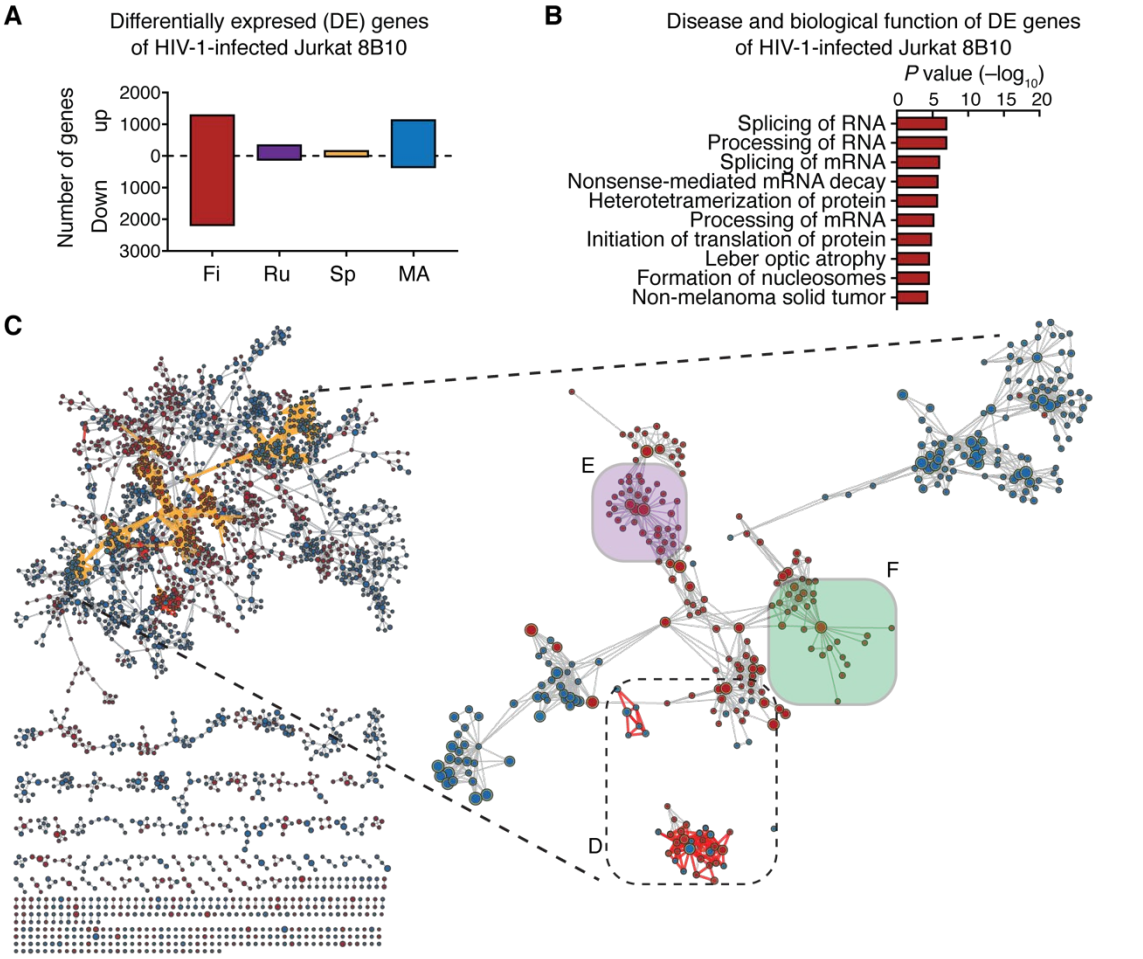
A
Differentially expresed (DE) genes
of HIV-1-infected Jurkat 8B10
Number of genes
up
Down
2000
1000
0
1000
2000
3000
Fi
Ru
Sp
MA
B
Disease and biological function of DE genes
of HIV-1-infected Jurkat 8B10
P value (–log10)
0 5 10 15 20
Splicing of RNA
Processing of RNA
Splicing of mRNA
Nonsense-mediated mRNA decay
Heterotetramerization of protein
Processing of mRNA
Initiation of translation of protein
Leber optic atrophy
Formation of nucleosomes
Non-melanoma solid tumor
C
E
F
D

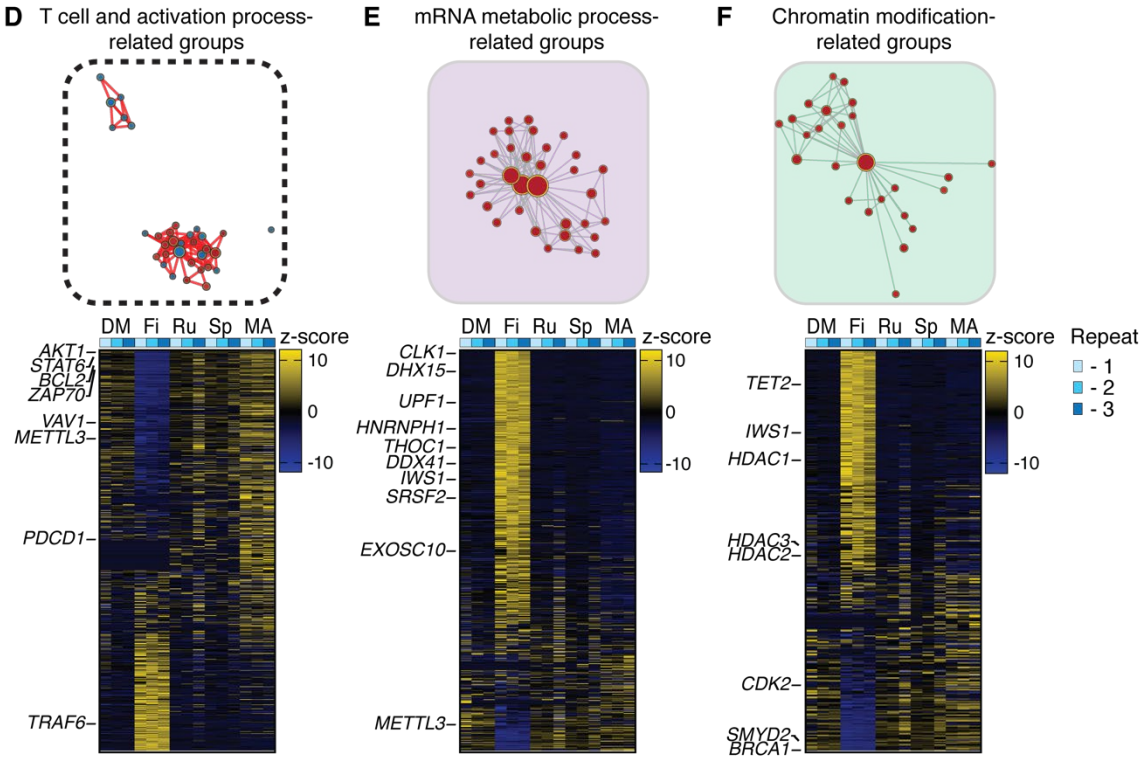
D T cell and activation process-related groups
E mRNA metabolic process-related groups
F Chromatin modification-related groups
DM Fi Ru Sp MA
z-score
10
0
-10
AKT1
STAT6
BCL2
ZAP70
VAV1
METTL3
PDCD1
TRAF6
CLK1
DHX15
UPF1
HNRNPH1
THOC1
DDX41
IWS1
SRSF2
EXOSC10
METTL3
TET2
IWS1
HDAC1
HDAC3
HDAC2
CDK2
SMYD2
BRCA1
Repeat
- 1
- 2
- 3

Figure S5. Pathway enrichment analysis of HIV-1-infected Jurkat clone 8B10 treated with HIV-1-suppressing agents. (**A**) Differential gene expression analysis of HIV-1-infected Jurkat clone 8B10 treated with HIV-1-suppressing agents for 24 hours. (**B**) Disease and biological function pathway analysis of differential expressed genes using ingenuity pathway analysis (IPA)(75)). (**C**) Results of gene set enrichment analysis (GSEA)(76) with gene ontology (GO) gene sets visualized by EnrichmentMap (114) in Cytoscape. Each node represents one gene set in GSEA Molecular Signature Database (MSigDB) GO gene sets that is significantly enriched (false discovery rate (FDR) < 0.25). The size of the nodes represents the number of genes in each gene set. Color red represents a positive enrichment score and color blue represents a negative enrichment score. The edge (connected lines between nodes) represents the degree of gene overlap between nodes. The cutoff of overlap coefficient was set to 1. We identified enriched pathways from the top 14 nodes with >22 interactions each. The expression levels of T cell activation-related gene sets (**D**), RNA metabolic process-related genes (**E**) and chromatin organization-related genes (**F**) in triplicates of HIV-1-infecte Jurkat 8B10. All analyses were done in triplicates.

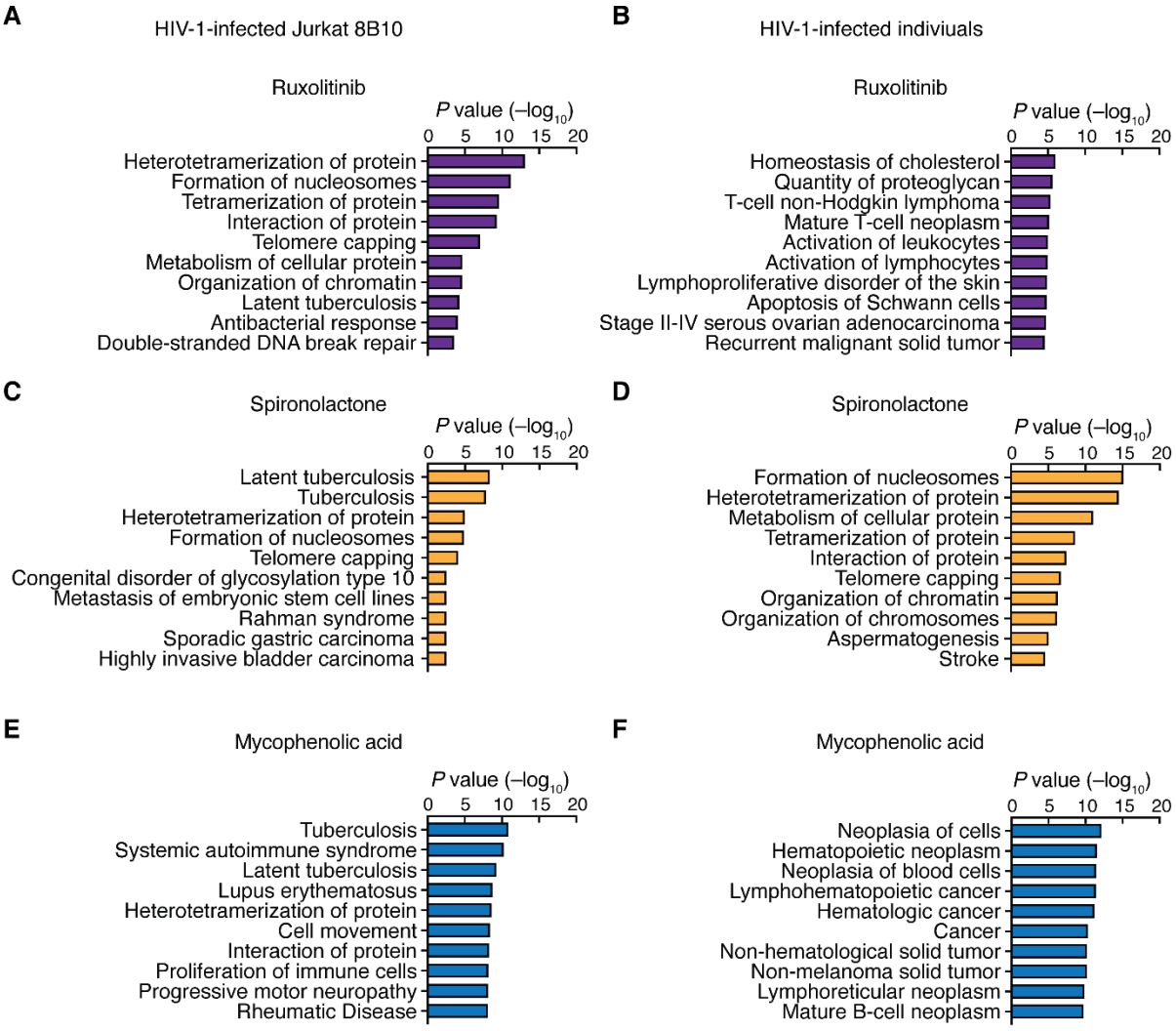

Figure S6. Pathway enrichment analysis using IPA on differentially expressed genes in HIV-infected Jurkat cell clone 8B10 and in CD4⁺ T cells from virally suppressed, HIV-1-infected individuals treated with ruxolitinib, spironolactone and mycophenolic acid. Data reflect triplicates of HIV-1-infected Jurkat 8B10 (**A, C, E**) and CD4⁺ T cells from three virally suppressed, HIV-1-infected individuals (HIV+ participants 1021, 1024, and 1025)(**B, D, F**) for 24 hours.

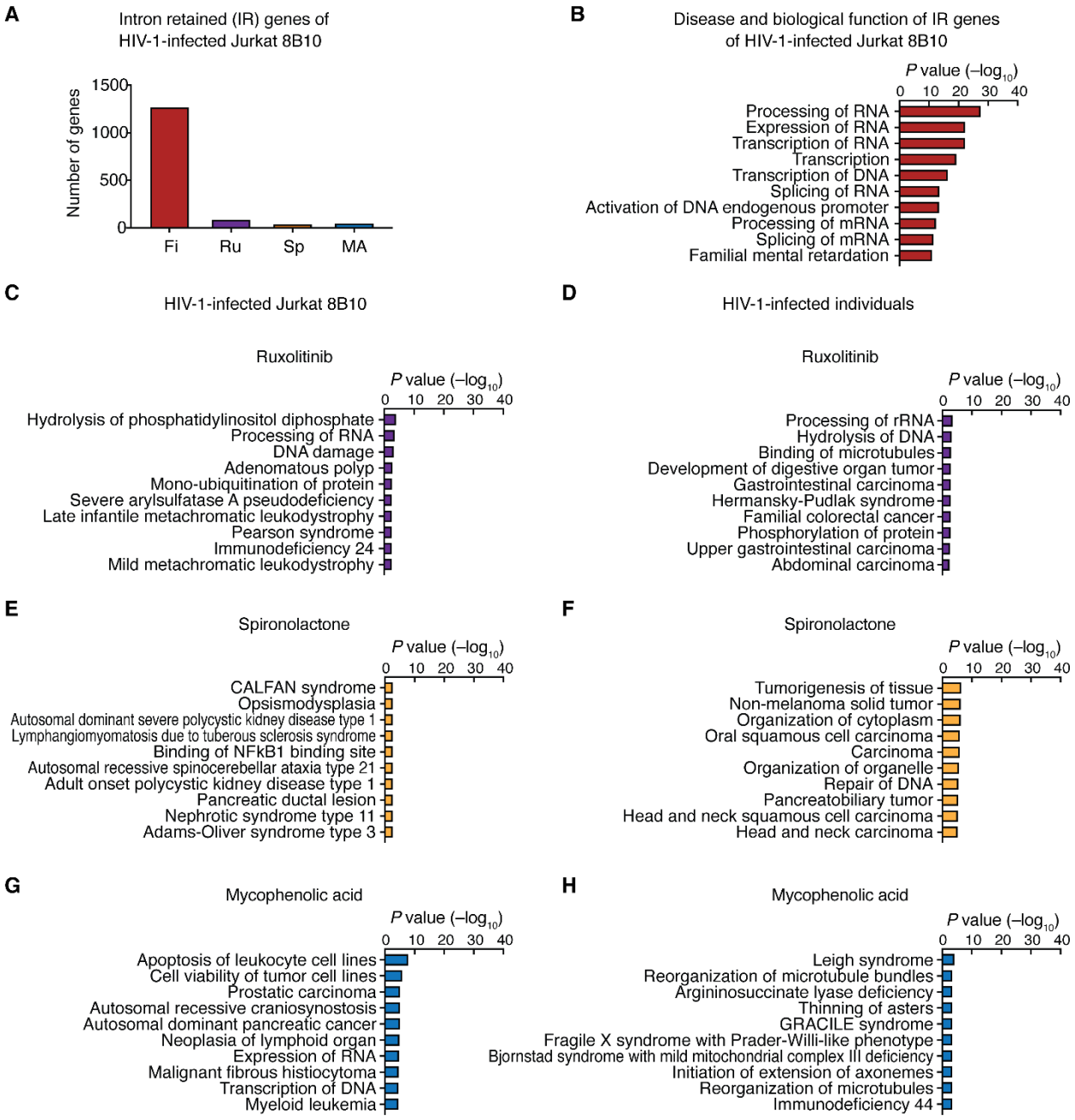

Figure S7. Intron retention analysis of HIV-1-infected Jurkat clone 8B10 and CD4⁺ T cells from virally suppressed, HIV-1-infected individuals treated with ruxolitinib, spironolactone and mycophenolic acid. (**A**) The number of intron-retained genes identified by IRFinder (77) in HIV-1-infected Jurkat 8B10 compared with DMSO-treated samples for 24 hours. Intron-retained regions with significantly increased ratio ($p < 0.05$, unequal variances *t*-

test) were reported. (**B**) Disease and biological function pathway analysis of intron retained genes using IPA in HIV-1-infected Jurkat 8B10 treated with filgotinib. Disease and biological functional pathway analysis using IPA demonstrated no significant pathway enrichment in ruxolitinib-treated (**C, D**), spironolactone-treated (**E, F**) and mycophenolic acid-treated (**G, H**) cell line and clinical samples (HIV+ participants 1021, 1024, and 1025).

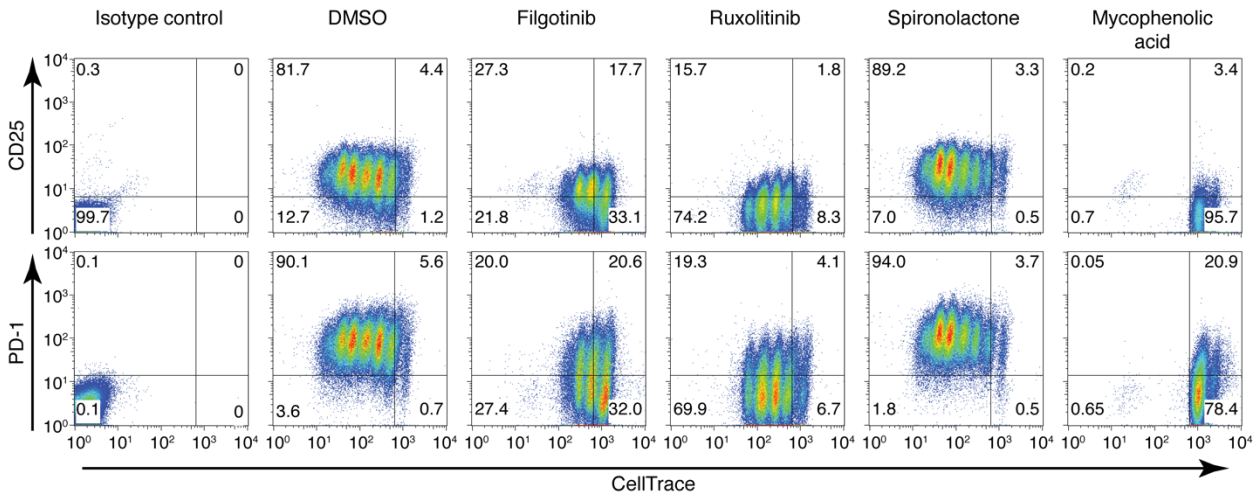

Figure S8. The effect of HIV-1-suppressing agents on T cell activation and cellular proliferation of CD4⁺ T cell from virally suppressed, HIV-1-infected individuals. CD4⁺ T cells from a virally suppressed, HIV-1-infected individuals were stained with CellTrace dye and treated with anti-CD3/CD28 magnetic beads in the presence of ART and respective HIV-1-suppressing agents for 3 days before flow cytometry analysis.

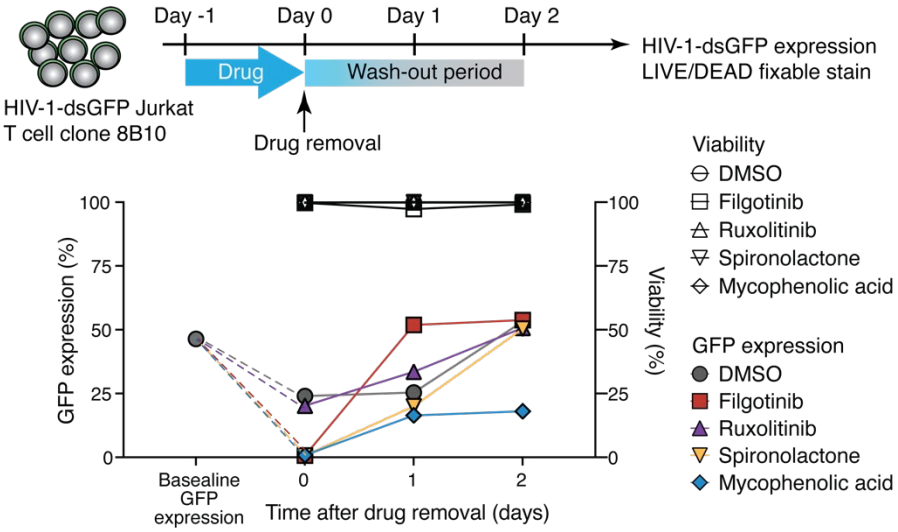

Figure S9. HIV-1-driven GFP expression levels after removal of HIV-1-suppressing agents removal. HIV-1-infected Jurkat clone 8B10 were treated with 10 μM HIV-1-suppressing agents for 24 hours. Agents were removed and GFP expression were measured by flow cytometry for two days. Cells viability were examined by staining with LIVE/DEAD dye.

Table S1. HIV-1-suppressing agents

HIV-1 suppressing agents	Mechanism of action
T cells activation	
JAK-STAT	
Filgotinib	JAK inhibitor selective for JAK1
Ruxolitinib	JAK inhibitor selective for JAK1/2
Receptor tyrosine kinase	
Dovitinib	Class III, IV and V receptor tyrosine kinase inhibitor
Pazopanib	VEGFR1/2/3, PDGFR, FGFR, c-Kit and c-Fms inhibitor
Ponatinib	Abl, PDGFRα, VEGFR2, FGFR1 and Src inhibitor
AKT	
Uprosertib	Akt inhibitor
Cation transport	
Digoxin	Na^+/K^+ ATPase inhibitor
Levosimendan	Calcium sensitizer
Zinc pyrithione	H^+ pump inhibitor
DNA unwinding process	
Topoisomerase	
Irinotecan	Topoisomerase I inhibitor
Mitoxantrone	Topoisomerase II inhibitor
DNA crosslinking	
Mitomycin C	DNA crosslinker
DNA helicase	
Spironolactone	XPB ATP-dependent DNA helicase (a part of the TFIIH transcription factor complex) inhibitor
RNA synthesis	
De novo guanosine triphosphate synthesis	
Mycophenolic acid	IMPDH inhibitor
Transcription elongation	
Flavopiridol	CDK1, CDK2, CDK4, CDK6, and CDK9 inhibitor
RNA splicing	
Filgotinib	New function identified in this study
RNA nuclear export	
KPT-330	RNA transport inhibitor selective for CRM1

CDK, cyclin-dependent kinase; CRM1, chromosomal maintenance 1; VEGFR, vascular endothelial growth factor Receptor; PDGFR, platelet-derived growth factor receptor; FGFR, fibroblast growth factor receptor; JAK, Janus kinase; IMPDH, Inosine-5′-monophosphate dehydrogenase

Table S2. Characteristics of study participants

ID	Age	Sex	Ethnicity	Current ART	Viral load (copies/ml)	Duration on ART (month)	Duration of undetectable viral load (month)
159	57	M	AA	ABC/DTG/3TC	<50	77	77
430	60	M	AA	ABC/3TC, EFV	<50	184	140
PH029	45	M	AA	ABC/DTG/3TC	<50	33	31
1001	50	M	AA	FTC/ RPV/TAF	<20	81	75
1002	47	M	AA	FTC/RPV/TDF	<20	282	51
1003	60	M	AA	BIC/TAF/FTC	<20	290	53
1004	59	M	AA	EVG/COBI/FTC/TAF	<20	222	119
1005	52	M	AA	ABC/DTG/3TC	<20	102	43
1006	54	F	AA	DRV, RTV, RAL	<20	384	72
1007	62	M	AA	FTC/RPV/TDF	<20	234	10
1008	64	M	AA	DTG/FTC/TAF	29.6	354	58
1009	57	M	AA	ABC/DTG/3TC	<20	230	89
1010	53	F	AA	ABC/DTG/3TC	<20	198	38
1011	56	F	AA	EFV/FTC/TDF	<20	62	18
1015	55	M	W	DRV/COBI, DTG/RPV	<20	386	19
1017	58	M	W	ABC/3TC, RAL, LPV/r	<20	410	16
1019	54	F	AA	ABC/DTG/3TC	<20	156	21
1021	68	M	AA	ABC/3TC, ATV	<20	194	21
1024	38	M	W	FTC/RPV/TAF	<20	88	75
1025	47	M	W	FTC/RPV/TAF	<20	68	57
1026	68	M	AA	FTC/TDF, RAL	<20	292	77
1035	67	F	AA	EFV/FTC/TDF	39.9	326	83
1036	62	F	AA	EFV/FTC/TDF	<20	158	85
1037	59	M	AA	ABC/DTG/3TC	<20	254	43
1039	54	M	H	ABC/DTG/3TC	<20	149	28
1049	53	F	W	BIC/TAF/FTC	<20	169	165
1053	62	M	AA	BIC/TAF/FTC	<20	328	310
UCSF2006	68	M	W	ABC/DTG/3TC	<40	253	238
UCSF2147	62	M	Asian	BIC/FTC/TAF	<40	246	172

AA, African American; H, Hispanic; W, White/Caucasian

3TC, lamivudine; ABC, abacavir; ATV, atazanavir sulfate; BIC, bictegravir; COBI, cobicistat; DRV, darunavir ethanolate; DTG, dolutegravir; EVG, elvitegravir; FTC, emtricitabine; LPV, lopinavir; LPV/r, lopinavir/ritonavir; RAL, raltegravir; RPV, rilpivirine; RTV, ritonavir; TAF, tenofovir alefenamide; TDF, tenofovir disoproxil fumarate